Biochimica et Biophysica Acta 1838 (2014) 2380–2390

Contents lists available at ScienceDirect

Biochimica et Biophysica Acta

journal homepage: www.elsevier.com/locate/bbamem

Dynamic membrane structure induces temporal pattern formation

J. Lippoldt *, C. Händel, U. Dietrich, J.A. Käs

Division of Soft Matter Physics, Faculty for Physics and Earth Sciences, University of Leipzig, Linnéstraße 5, 04103 Leipzig, Germany

ARTICLE INFO

Article history:
Received 27 January 2014
Received in revised form 5 May 2014
Accepted 16 May 2014
Available online 24 May 2014

Keywords:
Myristoylated electrostatic switch
Temporal pattern formation

ABSTRACT

The understanding of temporal pattern formation in biological systems is essential for insights into regulatory processes of cells. Concerning this problem, the present work introduces a model to explain the attachment/detachment cycle of MARCKS and PKC at the cell membrane, which is crucial for signal transduction processes. Our model is novel with regard to its driving mechanism: Structural changes within the membrane fuel an activator–inhibitor based global density oscillation of membrane related proteins. Based on simulated results of our model, phase diagrams were generated to illustrate the interplay of MARCKS and PKC. They predict the oscillatory behavior in the form of the number of peaks, the periodic time, and the damping constant depending on the amounts of MARCKS and PKC, respectively. The investigation of the phase space also revealed an unexpected intermediate state prior to the oscillations for high amounts of MARCKS in the system. The validation of the obtained results was carried out by stability analysis, which also accounts for further enhanced understanding of the studied system. It was shown, that the occurrence of the oscillating behavior is independent of the diffusion and the consumption of the reactants. The diffusion terms in the used reaction–diffusion equations only act as modulating terms and are not required for the oscillation. The hypothesis of our work suggests a new mechanism of temporal pattern formation in biological systems. This mechanism includes a classical activator–inhibitor system, but is based on the modifications of the membrane structure, rather than a reaction–diffusion system.

1. Introduction

Temporal patterns are intriguing features of biological systems, as they are assigned to regulate associated processes. For example, it has been reported that cytosolic calcium oscillations are essential for gene expression, as some genes can only be expressed in the presence of large amounts of calcium at a peak of the calcium oscillation [13,7]. The mechanisms behind the formation of such phenomena are of great interest because they give insights into the functionality of biological systems. While spatio-temporal pattern formation is discussed extensively for biological systems, the focus is mostly on reaction–diffusion systems and Turing pattern [45,19,34,28,43]. There have been only a few contributions investigating possible different mechanisms or purely temporal patterns, although new results in this thematic could have a great significance for the understanding of biological systems. In the present work, a new model with such an alternative mechanism was developed for experimentally observed density oscillations in an in vitro system, composed of proteins of a mammalian regulatory process — the myristoylated electrostatic switch (ME-switch).

The ME-switch regulates the membrane association of MARCKS (Myristoylated Alanine-Rich C Kinase Substrate) by phosphorylation involving PKC (protein kinase C) [44,36]. The interest in this mechanism is motivated by the contribution of MARCKS in numerous processes like brain development, cellular migration and adhesion, cytosis, neurosecretion, mitogenesis and regulation of the actin cytoskeleton [41,6]. It can bind to actin, calcium-activated calmodulin (Ca^{2+}/CaM), and the plasma membrane [24,21]. For the later, two interactions are required: hydrophobic interactions between the myristolated N-terminus of MARCKS and the membrane as well as electrostatic interactions between the positively charged effector domain and acidic lipids within the membrane (Fig. 1). The membrane binding of the effector domain sequester acidic lipids like PIP_2 (phosphatidylinositol 4,5-bisphosphate) [20], which is a well known component of mammalian plasma membranes involved in signal transduction processes [9]. The membrane bound effector domain is also the target for Ca^{2+}/CaM binding and phosphorylation by PKC. Both of these processes are independent from one another and prevent a further membrane association of MARCKS until they are reversed in the cytosol [24].

The experimentally difficult access to such complex interactions at the cell membrane motivates the development of mathematical models. A model, concerning the ME-switch was developed by John et al. [26]. It was calculated that molecular interactions between proteins and membrane lipids can induce pattern formation in cell membranes and a coupling exists between the protein induced phase separation and reaction–diffusion processes. An experimental access to this system was found by Langmuir-monolayer technique [2]. The investigated system consisted of a mixed monolayer with DPPC (1,2-dipalmitoyl-sn-glycero-3-phosphocholine) as matrix lipid and PIP_2 (1,2-dipalmitoylphosphatidylinositol 4,5-diphosphate) as

* Corresponding author. Tel.: +49 341 97 32486; fax: +49 341 97 32479.
E-mail address: juergen.lippoldt@uni-leipzig.de (J. Lippoldt).

http://dx.doi.org/10.1016/j.bbamem.2014.05.018
0005-2736/

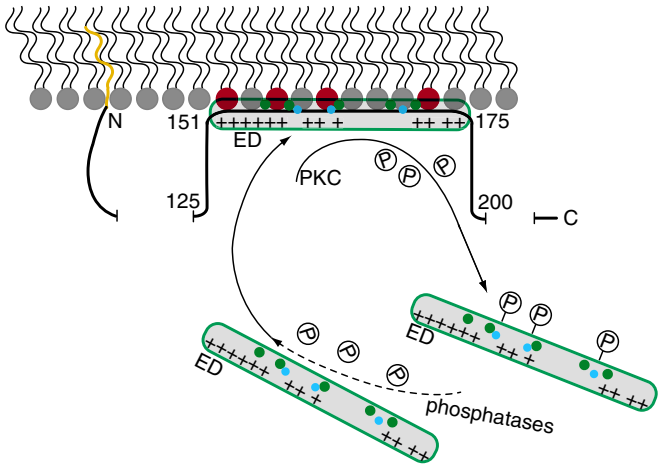

Fig. 1. MARCKS binds to a lipid membrane via hydrophobic interactions at his N-terminus and electrostatic interactions between its strongly positively charged effector domain and acidic lipids within the membrane. A phosphorylation of serines in the effector domain by PKC inhibits a further membrane attachment until the molecule is dephosphorized in the cytosol.

negatively charged membrane lipid. DPPC was used as matrix lipid, as it features a state of phase coexistence of a fluid and a crystalline phase mimicking structural inhomogeneities in cell membranes [9]. Furthermore, there are adequate reference data, important for separating particular lipid contributions in the mixture [15,1]. The ME-switch, essentially based on the electrostatic interaction of PIP_2 with MARCKS, was mimicked by an excess of unphosphorylated MARCKS in the subphase and an injection of protein kinase C into the subphase [2]. The attachment of unphosphorylated MARCKS at the monolayer was detected by an increase of the lateral pressure of the monolayer, while the detachment, caused by the phosphorylation of MARCKS by PKC, was measured by a decrease of the lateral pressure of the monolayer. The changes of the lateral pressure were attributed to concentration dependencies of membrane bound MARCKS. This in vitro measurement showed the development of temporal patterns of the ME-switch in terms of a low frequency density oscillation of membrane bound MARCKS [2].

Based on these experimental results, an empirical model was developed by Alonso et al., which explains the observed oscillation by means of structural changes within the membrane [2]. Here, the initial ansatz is a simple approach to predict the oscillation of the lateral pressure of the monolayer, starting from a reduced number of parameters to a particular choice of non-linear functions for the reaction rates, based on general arguments. It sketched out an interplay of electrostatic interactions between the reactants, the changing binding probability of the proteins and the change of the mean molecular area requirement within the membrane interface, which results in an oscillatory behavior of the lateral pressure of the monolayer. For a complete characterization of this process further experimental studies are necessary. Nevertheless, there are a lot of parameters which have strong and significantly different influences on the attachment/detachment cycle of MARCKS and PKC at the cell membrane. On this account, we were motivated to develop a new model on the basis of the model of Alonso et al. [2] in order to be able to predict the experimental conditions at which the oscillatory behavior occurs. Our model allows to obtain more detailed statements about the dependency of the adjustable parameters in the considered attachment/detachment cycle. Thereby it enables further specific experimental studies and may in the long run contribute to a better understanding of regulation processes like the ME-switch. Furthermore, the crucial assumption that PIP_2 localizes in the disordered phase is validated by epifluorescence measurements in this publication. Besides strengthening the models, these measurements provide a basis for further visualizations and microscopic studies of membrane related temporal pattern formations.

Our model is formulated in a system of nonlinear differential equations and is solved numerically with the finite difference method. Structural changes of the membrane were specified with an empirical equation, according to the previous experimental results, obtained by Alonso et al. [2]. The involved chemical reactions and attachment detachment processes were analyzed with respect to a better adaptation to the experimental conditions, leading to a good approximation for biological systems. The influence of critical parameters was estimated by their variations. Based on this result, phase diagrams were generated to illustrate the interplay of MARCKS and PKC. They describe the oscillatory behavior by the number of peaks, the periodic time, and the damping constant depending on the amount of MARCKS and PKC, respectively. Thus, our model can predict the development of oscillations in the observed system depending on the amount of the reactants.

In order to achieve an approximation for biological systems, the process is also analyzed as an open system. Thereby diffusion is neglected. The fact that this does not prevent the oscillation from occurring points out that the oscillation is not caused by a classical reaction–diffusion mechanism. It is rather induced by the mutual interaction of the membrane structure and protein binding to the membrane.

2. Theory

2.1. Mechanism of oscillation

The here discussed mechanism of temporal pattern formation originates from an activator–inhibitor system driven by a changing membrane structure. The membrane investigated in the underlying experiments was composed of lipids within the phase transition between liquid expanded and liquid condensed phase (alternatively named disordered and ordered phase). The binding of proteins on the membrane changes the structure of the membrane which feeds back on the attachment rates of proteins. The dependency of the attachment rate of PKC on the membrane structure is higher than for MARCKS. As PKC detaches MARCKS from the membrane and the presence of MARCKS at the membrane enhances PKC attachment, an activator–inhibitor system is formed. The time delay, necessary for an oscillation, is caused mainly by the time the membrane needs to restructure after protein binding.

Fig. 2 provides a visualization of the processes during each phase of the oscillation. The left part of the figure illustrates the membrane structure and amount of membrane bound proteins during each phase. The right part of the figure shows the time evolution of these observables. Fig. 2a: With a low amount of proteins attached to the membrane, the amount of disordered phase is rather low which is also reflected in the variable membrane state θ'. Fig. 2b: Over time MARCKS attaches to the disordered phase, thereby increasing its proportion. Fig. 2c: The increased size of the liquid disordered phase enhances the attachment of MARCKS as well as PKC, but the attachment of PKC leads to phosphorylation and detachment of MARCKS. Fig. 2d: The shrinking amount MARCKS reduces the size of the disordered phase, which in turn decreases the amount of membrane bound PKC, due to an attachment–detachment equilibrium.

2.2. Modeling of the ME-switch

The modeling of Alonso et al. has demonstrated, that the experimentally observed oscillation of the lateral pressure of the monolayer can be explained theoretically [2]. However, it cannot provide a correct description of all experimental details. Thus, we have developed a new model which allows to predict the behavior of the observed system – the ME-switch – dependent on system relevant parameters like the amount of MARCKS and PKC, respectively. The fundamental structure of the model of Alonso et al. was preserved.

In the underlying experiments homogeneous density oscillations within the membrane have been observed. Therefore the lateral

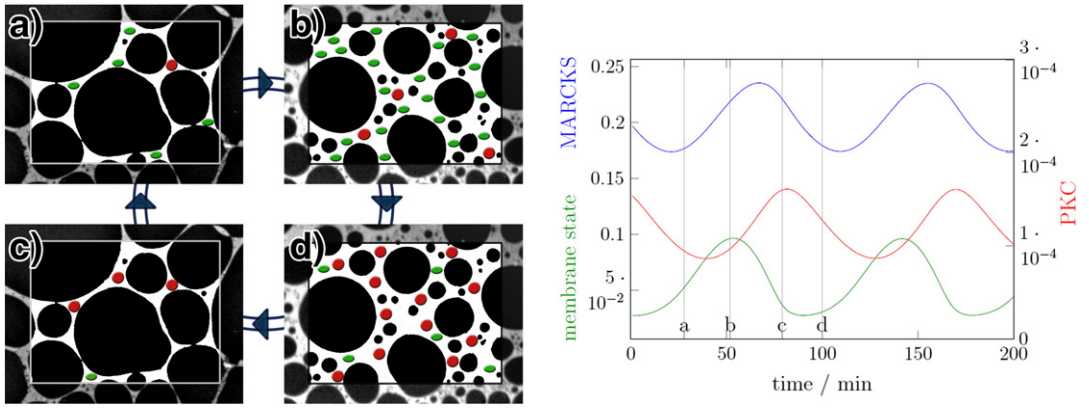

Fig. 2. The left figure is a sketch, illustrating the membrane structure and protein attachment during different phases (a–d) of the oscillation. The bright parts of the background symbolize the disordered phase of the membrane and the dark parts the ordered phase. The green dots indicate MARCKS molecules while the red dots stand for PKC. The right figure shows the membrane associated variables' amount of membrane bound 'MARCKS m' in green, the 'amount of membrane bound PKC p' in red and the 'membrane state θ' in blue during an simulated oscillation within an open system. The time evolution of the observables is matching the left sketch.

dimension of the membrane is disregarded and only the perpendicular direction $0 < z < L$ is treated. This approach models the spatial averaged concentration of the reactants. The variables of the model are the amount of MARCKS in the fluid phase M and bound to the membrane m, the amount of PKC in the fluid phase P and bound to the membrane p, the amount of phosphorylated MARCKS M_p in the fluid phase as well as the state of the membrane θ, which treats the ability of the membrane to bind the reactants. The amount of protein is normalized to one for a completely covered membrane. A protein can bind to the membrane during a time frame Δt, when it is previously within a small layer of thickness l close to the membrane. The introduction of the layer $0 < z \leq l$ is helpful to discretize the problem for a proper use of a finite difference algorithm. Thereby the attachment rates are averaged over time and initial distance to the membrane corresponding to a Robin boundary condition [17], while the detachment rates are first order kinetics. This is just a discretization approach and the mesh size l is chosen so small that a further reduction has no effect. The following equations arise for $0 < z \leq l$:

$$\begin{aligned} \partial_t M(z,t) &= D_M \partial_z^2 M(z,t) - R_M \\ \partial_t P(z,t) &= D_P \partial_z^2 P(z,t) - R_P \\ \partial_t M_P(z,t) &= D_M \partial_z^2 M_P(z,t) + R_{MP} \end{aligned} \tag{1}$$

where D_M and D_P are the diffusion coefficients of MARCKS and PKC and $R_i(t)$ are the nonlinear reaction terms, which account for the attachment/detachment of the proteins to the membrane and the phosphorylation of MARCKS by PKC. They are dependent on the concentration of MARCKS and PKC close to and on the membrane as well as the membrane structure. If the protein is not close to the membrane ($z > l$), the reaction terms are zero. For the time-evolution of the membrane bound reactants, the following equations arise:

$$\begin{aligned} \dot{m}(t) &= R_M(t) - R_{MP}(t) \\ \dot{p}(t) &= R_P(t). \end{aligned} \tag{2}$$

In the case of the relevant closed system, the total amounts of PKC $P_0 = \int_0^L (z,t)dz + p(t)$ and MARCKS $M_0 = \int_0^L (M(z,t) + M_p(z,t))dz + m(t)$ are preserved quantities, while unphosphorylated MARCKS is transformed to phosphorylated MARCKS by PKC (R_{MP}).

The detachment kinetic of MARCKS and PKC is assumed as a first order kinetic. For the attachment of MARCKS, a first order kinetic with respect to the membrane state θ was applied, in agreement to [3,48]. For the attachment of PKC at the membrane, a cooperative kinetic regarding the membrane state θ was used. Thereby a cooperativity coefficient of $n_{PKC} = 4$, is consistent with studies reporting a cooperative binding with respect to the proportion of active lipid [14,31,32]. The phosphorylation of MARCKS by PKC occurs with a cooperative kinetic, according to [22]. For this reaction a cooperativity coefficient of $n_{phos} = 3$ was assumed [22]. This leads to the following reaction terms:

$$R_M(t) = \theta \; k_m^+ \; M(l,t) - k_m^- \; m(t) \tag{3}$$

$$R_P(t) = \frac{k_p^+ \; \theta^4}{K_2^4 + \theta^4} \; P(l,t) - k_p^- \; p(t) \tag{4}$$

$$R_{MP}(t) = \frac{v_{max} \; p(t) \; m(t)^3}{S_0^3 + m(t)^3}. \tag{5}$$

The membrane state θ plays a crucial role for the attachment of proteins at the membrane. The enrichment of charged lipids in the disordered phase facilitates the lipid/protein interaction in this phase. Hence, the proportion of disordered phase strongly influences the attachment rate of proteins. The proportion of disordered phase enters the membrane state in a square root, as the diffusive binding constant of a particle to a disk is proportional to the radius [42]. The MARCKS attachment increases the proportion of the disordered phase [2,11]. For this dependency we have used an empiric equation, which states that the proportion of a disordered phase increases proportional to the amount of membrane bound MARCKS from an initial amount. It should be noted, that the structure of the membrane needs time to adjust to the binding of MARCKS, which is accounted for by the constant k_θ in Eq. (6). Another effect to consider is the screening of lipids by the membrane bound proteins, which occurs instantaneously.

$$\dot{\theta}_{st}(t) = k_\theta \left(\left(\sqrt{A_{dis} m(t)} - \theta_{st} \right) \right) \tag{6}$$

$$\theta = (1 - m(t))(1 - p(t))\theta_{st}. \tag{7}$$

2.3. Determination of parameters

The MARCKS effector domain (MARCKS (151-175)), which is responsible for the electrostatic interaction with the cell membrane [4,47,38], substitutes MARCKS in the underlying experiment [2]. This peptide consists of 25 amino acids with 13 basic residues and is rod-shaped in an aqueous environment [6]. An approximation for the hydrodynamic radius of rod-shaped molecules was given by He and Niemeyer [25]. With the radius and the length of the cylinder, approximated by the

average radius of the amino acid residues, the hydrodynamic radius of MARCKS (151-175) was estimated and applied in the Stokes–Einstein equation to calculate the diffusion coefficient of MARCKS peptides: $D_M = 215\,m^2 s^{-1}$. The hydrodynamic radius of PKC was obtained from a Sigma data sheet (product code P 7956). According to the Stokes–Einstein equation, the following diffusion coefficient results for PKC: $D_P = 51\,m^2 s^{-1}$.

The maximal attachment rates of MARCKS k_m^+ and PKC k_p^+ are limited by diffusion [4,40,39]. In order to adapt this for the finite difference method, the maximal attachment rates were calculated with a self written Matlab algorithm. The diffusion limited attachment rate was approximated by the proportion of reactants which reach the membrane in a diffusive process out of the closest grid box in a given time frame. This time frame is the time in which the 3σ-environment of the closest point outside the first grid box reaches the membrane. The resulting attachment rates are dependent on the t-grid size and the x-grid size, of the finite difference algorithm, and have to be evaluated again if the grid sizes are changed. Here, the usually applied x-grid size is $x_{grid} = 10$ m and the t-grid size is $t_{grid} = 0.025$ s. The following attachment rates result:

$$k_m^+ = 0.259\,s^{-1} \qquad k_p^+ = 0.127\,s^{-1}.$$

In a diffusive process, the characteristic time increases with the square root of time. Thus, the amount of reactant which diffuses to the membrane increases with a square root relation with respect to time. Since every other metric in this model is linear with respect to time, the maximal attachment rates are normalized to a linear metric by division by t_{grid}.

The dissociation constant of MARCKS is $k_m^- = 1\ s^{-1}$ [48] and of PKC is $k_p^- = 0.42\ s^{-1}$ [39]. These parameters were measured with a PIP_2 concentration of 1%. This is on the lower end of the physiological level (1%–5% [6]) and much lower than in the discussed experiment, where a concentration 10% was used. By isotherm and fluorescence measurements of mixed monolayers containing different amounts of PIP_2, it could be found that 10% of PIP_2 has no significant influence on the DPPC matrix. Experiments with lower concentrations of PIP_2 than 10% did not prove suitable to observe significant effects in a noisy macroscopic film balance experiment. In addition, PIP_2 is concentrated in the disordered phase, which moreover increases its concentration in this area. The concentration of acidic lipids distinctly changes the lifetime of membrane attached peptides. It can be expected that the dissociation constants in the current experiment are much lower than stated above. Indeed, the dissociation constants have to be much lower to reproduce the experimental results. The finally applied parameters are $k_m^- = 0.003\ s^{-1}$ for MARCKS peptide and $k_p^- = 0.00084\ s^{-1}$ for PKC.

The parameter K_2 represents the value on which the attachment rate of PKC is the half of its maximum. For this parameter, suitable reference values could not be found. The adjustment of the parameters in order to reproduce the experimental results leads to a value of $K_2 = 1.7$. For k_θ, which accounts for the time of reorganization of a membrane after MARCKS binding, the value applied in [2] was taken as orientation. Finally, the value amounts to $k_\theta = 0.0007\ s^{-1}$. The maximum phosphorylation rate of MARCKS by PKC was measured as $v_{max} = 2(\text{molMARCKS})(\text{s mg PKC})^{-1}$ [21]. This value was used without the modification and the conversion into internal units of the model results in $v_{max} = 5.33\ s^{-1}$. The concentration of MARCKS at the membrane, which leads to a half maximum enzymatic activity of PKC, was found out with $S_0 = 20$ nm [21]. This corresponds to $S_0 = 0.8$ in the internal units of the model. However, this parameter was measured in the presence of lipid vesicles. Contrary to this reference, the concentration of MARCKS in the modeled experiments is clearly enhanced due to its enrichment in the disordered phase. Thus, the actual value results from the adjustment as $S_0 = 0.015$. The concentration of MARCKS M_0 and PKC P_0 in the subphase is chosen in the range of the conditions of the underlying experiment [2]. The determined parameters are depicted in Table 1.

3. Experimental background

3.1. Materials

1,2-Dipalmitoyl-sn-glycero-3-phosphatidylcholine (DPPC, 85035 5P) was obtained from Avanti Polar Lipids (Alabaster, USA) and BODIPY labeled phosphatidylinositol 4,5-bisphosphate (PIP_2, C-45F6a) from Echelon (Salt Lake City, USA). Phosphatidylinositol 4,5-bisphosphate (PIP_2, P7115) was purchased from Sigma-Aldrich (Germany). All lipids are saturated in order to ensure a stable conformation during the large periods of measurement times. Furthermore, both membrane lipids have the same chain length to avoid a mismatch between the lipids caused by different sizes. Potential disturbances by the Marangoni effect are prevented by the relatively large chain length [35]. NaCl (S7653), HEPES (H3375) and EDTA (E4884) were purchased from Sigma-Aldrich (Germany), chloroform and methanol form Merck (Darmstadt, Germany) and Rhodamine DHPE (L-1382) from Invitrogen (Karlsruhe, Germany).

3.2. Methods and experiments

Numerous experimental evidences concluded an enrichment of negatively charged lipids in the liquid expanded phase of biomimetic membranes due to their repulsive electrostatic interactions [33,12,37]. By means of fluorescence microscopy, an increase of the liquid expanded phase during the MARCKS (151-175) attachment to a DPPC/PIP_2 membrane was interpreted as a MARCKS (151-175)/PIP_2 complex formation within the disordered phase [47,11,23]. The following experiments directly validate these experimental observations with fluorescent labeled PIP_2.

In the present experiments we prepared model membranes above the main phase transition between the ordered and disordered phases. Mixed DPPC/PIP_2 monolayers were used, whereby DPPC acts as matrix for the PIP_2 molecules. In order to study the lateral organization of the charged PIP_2 in a lipid membrane, monolayer experiments were performed using Langmuir trough technique. Monolayers at the air–water interface are well-established biomimetic membranes, which offer large observation areas and give an insight in the lateral organization of lipid membranes on a micrometer scale. Because of their controllable parameters, monolayers are well defined systems and accessible by film balances combined with fluorescence microscopy.

Investigating the phase separation into a DPPC rich condensed phase and a PIP_2 rich disordered phase, we prepared monolayers composed of

Table 1
Description and values of the used parameters.

Amount of MARCKS $M_0 = 3$	Amount of PKC $P_0 = 0.02$
Diffusion constant of MARCKS $D_M = 215\ \mu m^2\ s^{-1}$ [6,25]	Diffusion constant of PKC $D_P = 51\ \mu m^2\ s^{-1}$
Attachment rate of MARCKS $k_m^+ = 0:259\,s^{-1}$ [4]	Attachment rate of PKC $k_p^+ = 0.127\,s^{-1}$ [39,40]
Detachment rate of MARCKS $k_m^- = 0:003\,s^{-1}$ [48]	Detachment rate of PKC $k_p^- = 0:00084\,s^{-1}$ [39]
Microscopic dissociation constant of PKC $K_2 = 1.7$	Amount of membrane bound MARCKS for half-maximal PKC activity $S_0 = 0.015$ [21]
Organization velocity of the membrane $k_\theta = 0.0007 s^{-1}$ [2]	Maximal phosphorylation rate $v_{max} = 5:33\ s^{-1}$ [21]
Spatial grid size $x_{grid} = 10$ m	Temporal grid size $t_{grid} = 0:025$ s

DPPC, PIP_2 and BODIPY labeled PIP_2 (molecular ratio 9:1:0.1). DPPC powder was dissolved in chloroform/methanol (4:1) in a concentration of about 0.5 g/*l* and the labeled and unlabeled PIP_2 was dissolved in chloroform/methanol/water (10:10:1) in a concentration of 0.1 g/*l*. As fluorescent labeled PIP_2 the 4,5-diphosphatic derivate of the inositol molecule was chosen from the variety of the labeled PIP_2 molecules being identical to the inositol derivate present in the unlabeled PIP_2. The counter ions are ammonium in the case of the unlabeled and triethylammonium for the labeled one. According to the manufacturer this does not significantly influence the behavior of PIP_2, since the dissociated species are investigated.

Furthermore we performed control experiments with mixed DPPC/unlabeled PIP_2 monolayers (molecular ratio 9:1). The mixed monolayers in the control experiment contained 1.0 mol% Rhodamine DHPE to visualize the lateral phase separation into a DPPC rich condensed phase and a dye rich disordered phase.

The mixed DPPC/PIP_2 solutions were spread on buffer solutions and the solvent could evaporate for at least 10 min. The subphase was composed of 100 mM NaCl, 10 mM HEPES and 0.1 mM EDTA. The chemicals of the subphase were dissolved in ultra pure water obtained from a Milli-Q system ($\rho > 18\ M\Omega\ cm$) and the buffer was adjusted to pH 7.4. The monolayers were compressed with a film balance from KSV instruments (Minimicro LB system, Helsinki, Finland) at a subphase temperature of 22 °C and a barrier speed of approximately 2 $Å^2$/(molecule min) to a target pressure of $\pi = 10$ mN/m, where the monolayer is in a state of phase coexistence. The investigation of the mesoscopic morphology of the monolayers was performed with an epifluorescence microscope from Olympus, Japan.

3.3. Fluorescence microscopy of DPPC/PIP_2 monolayers

The lateral distribution of the negatively charged acidic lipid PIP_2 in biomimetic membranes is visualized by fluorescence microscopy. Fig. 3 shows fluorescence micrographs of the mixed DPPC/PIP_2 monolayers at a surface pressure of 10 mN/m at 22 °C. Indeed this pressure is lower than the physiologically relevant value of 30 mN/m [8]. However, at 10 mN/m the monolayer consists of a condensed highly packed state (dark) in coexistence with disordered loosely packed regions (bright) — comparable to cell membranes. At this lateral pressure the lipid domains are well distinguishable. The lateral organization of pure DPPC monolayers is a well understood system and serves as starting point of our experiments [15,27].

In prior publications, the enrichment of PIP_2 in the disordered phase of a DPPC matrix was a conclusion of strong experimental hints. The repulsive electrostatic behavior of PIP_2 molecules and an increased area of disordered phase if MARCKS (151-175) peptides interact with a mixed DPPC/PIP_2 membrane, however, provide strong evidence [11,33]. Due to the previous experiments we assume that Fig. 3a shows a lateral phase separation into a DPPC rich condensed phase and a PIP_2 enriched disordered one.

Fig. 3b shows a fluorescence micrograph with BODIPY labeled PIP_2 within a DPPC matrix. The image shows a lateral phase separation into the DPPC rich phase (dark domains) in coexistence with a PIP_2 rich one (bright areas between the dark domains). This directly demonstrates an enrichment of labeled PIP_2 outside the condensed domains. The similarities in form and size between the domains in Fig. 3a and b strongly suggest that the dark domains in Fig. 3b correspond to the ordered phase of Fig. 3a. This produces evidence that PIP_2 is strongly enriched in the disordered phase of a lipid membrane and supports the assumptions of the model.

4. Results

4.1. A single simulated time evolution: validation and analysis

Fig. 4 shows that after an initial increase over the course of several hours, the amount of membrane bound MARCKS reaches a saturation level which constitutes an equilibrium between attachment and thermal detachment of MARCKS molecules. The comparatively large period of time is caused by an increase of the attachment rates over time, due to the structural changes of the membrane by MARCKS binding. Furthermore, the long diffusion times of MARCKS in the 5 mm deep trough, used in the experiments, have an influence, since the low detachment rates allow for a suction effect. Such suction effects do only occur in the large scale in vitro experiment and are not relevant for small systems like living cells. The saturation level of membrane bound MARCKS is dependent on the concentration of MARCKS in the subphase, with a maximal saturation level, where nearly all PIP_2 in the membrane is bound. These maximal saturation levels equal 1 in the internal units of the model.

Our model, particularly the absence of a time delay between the initial decrease of the amount of membrane bound MARCKS and the starting oscillation, describes experimental observations well. The sharp transition from the initial decrease of membrane bound MARCKS after the PKC injection to the following long-term behavior is well observed in the experiments. First, this was regarded as an experimental artifact, possibly due to convection effects based on the PKC injection [2], but it could well be a true feature of the system as these simulations indicate. Furthermore, it is remarkable that the oscillation is not influenced by the injection point of PKC m_i over a large range.

Fig. 5 shows the time evolution of the three membrane associated variables. The damped oscillations of these variables have the same periodic time of about three hours. A phase shift between these oscillations exists, while MARCKS peaks first. The membrane state is shifted

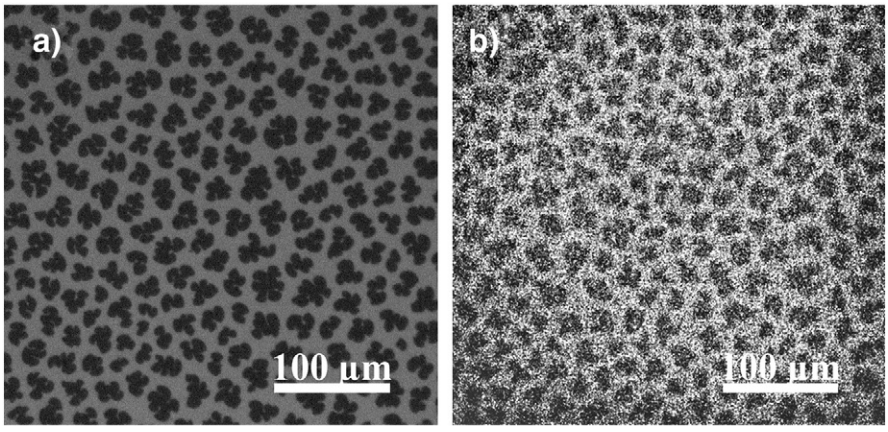

Fig. 3. Fluorescence micrographs of the monolayers (Olympus, Japan). a) DPPC/unlabeled PIP_2/Rhodamine DHPE mixture and b) DPPC/unlabeled PIP_2/BODIPY labeled PIP_2 mixture, both on the buffer solution described in Chapter 3.1 and at $\pi = 10 mN/m$, $T = 22°C$. The gamma setting has been adjusted.

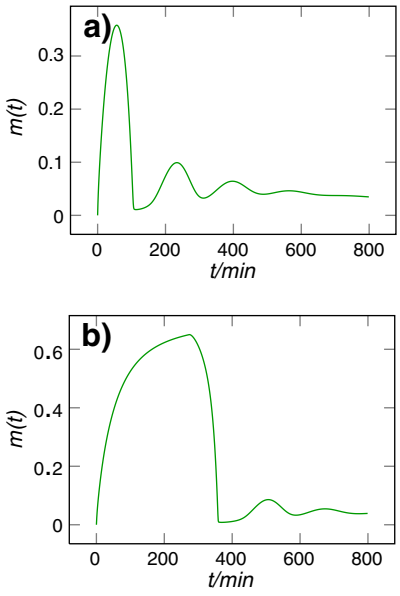

Fig. 4. $m(t)$ is the amount of membrane bound MARCKS, dependent on time. Similar to the underlying experiments, PKC was added to the system after some time in which MARCKS could attach on the membrane. This figure displays the behavior of our model by different PKC injection points. a corresponds to an injection at $m_i = 0.2$ and b to an injection at $m_i = 0.65$.

because the reorganization of the membrane structure after binding of MARCKS is not instantaneous. The increasing membrane state leads to an increased binding of PKC, whose phase is again shifted to later times. The increase of membrane bound PKC leads to the decrease of MARCKS on the membrane which lowers the membrane state, and ultimately yields a decrease of membrane bound PKC. The decrease of membrane bound PKC leads to an increase of the overall attachment rate of MARCKS, starting the next period of the oscillation. These oscillations are always damped because the amount of unphosphorylated MARCKS is exhausted during the experiment.

In the simulations, one can determine variables, which are inaccessible in experiments, like the distribution of reactants in the subphase. The concentration of unphosphorylated MARCKS in the subphase $M(t,z)$ has a minimum near the membrane, as there is a constant consumption of unphosphorylated MARCKS in the presence of PKC at the membrane. In a representative simulation, the concentration of MARCKS close to the membrane is about an eighth of the concentration at the

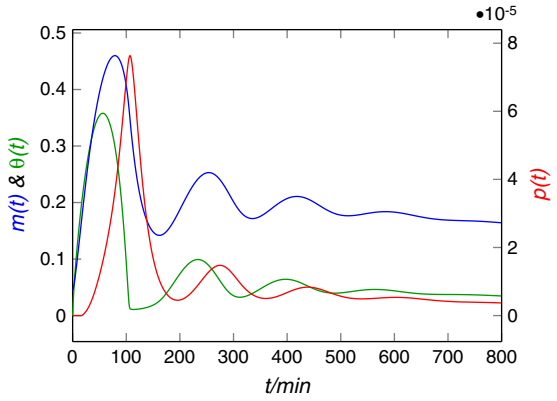

Fig. 5. Time evolution of the membrane associated variables in a single simulation of the closed system. The green curve is the amount of membrane bound MARCKS $m(t)$, the red is the amount of membrane bound PKC $p(t)$, and the blue is the membrane state $\theta(t)$. All of them are presented in the internal variables of the model. Since the amount of bound PKC is significantly lower then the other two values, it is presented in a different scale (right side of the diagram).

far end of the through. For PKC, one can state that the local differences in the concentrations are small, at a maximum of about 4%. This is caused by the slow alteration rates compared to the characteristic diffusive times. The PKC concentration in the subphase has maxima and minima corresponding to the oscillation of membrane bound PKC.

4.2. Phase diagrams

Fig. 6 illustrates the intensity of the oscillatory effect by plotting the number of oscillatory peaks which arise under certain initial conditions. The total amount of MARCKS M_0 and PKC P_0 was varied logarithmically around a reasonable initial value. It can be seen that the oscillations develop only at a certain relation of MARCKS to PKC. If the proportion of MARCKS is significantly higher than at those conditions, PKC has no major effect. In this case the phosphorylation rate is small compared to the thermal detachment rate of MARCKS. This causes a slightly increased effective detachment rate and a slow transformation of unphosphorylated MARCKS to phosphorylated MARCKS accompanied by a slow decrease of the saturation level of membrane bound MARCKS. In case of low amounts of MARCKS in the system, the phosphorylation rate is large compared to the attachment of MARCKS even for low amounts of PKC at the membrane. This prevents an increase of the amount of membrane bound MARCKS after its initial decrease caused by the addition of PKC. For high amounts of PKC the damping constant of the oscillatory effect increases, since more MARCKS get phosphorylated in the same time, which eventually leads to an over-damped oscillation.

The phase diagram in Fig. 6 is almost symmetric for the amount of PKC P_0 with long persistent oscillations. The oscillatory regime nearly has the appearance of a tilted ellipse in the logarithmic phase space, since lower amounts of PKC are needed for an oscillation if lower amounts of MARCKS are present. However, this shape does not evolve because the oscillatory region is cut off at a certain amount of MARCKS. The cut off is caused by an effect, which becomes apparent by examining the time evolution of membrane bound MARCKS $m(t)$ and PKC $p(t)$ near the cut off (see Fig. 7). For high MARCKS concentrations, the system enters a slow changing state prior to the initial decrease of bound MARCKS due to PKC injection. In this state, a high amount of MARCKS is bound to the membrane and reduces the binding of PKC by shielding a high amount of PIP_2. Thus, only a low amount of PKC can bind to the membrane and reduces the amount of bound MARCKS only very slowly until enough MARCKS is detached to allow for a significant increase of membrane bound PKC.

Fig. 8a shows the periodic time of the oscillations with more than 1 peak. It is clearly visible that the main factor for the periodic time of the oscillation is the amount of PKC P_0. The periodic time decreases for increasing amounts of PKC. The amount of MARCKS M_0 has a minor

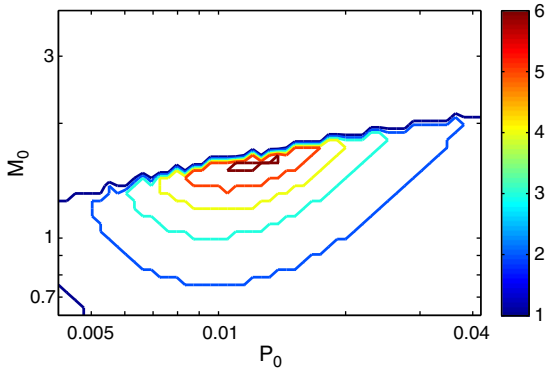

Fig. 6. Phase diagram of the closed system. P_0 is the total amount of PKC in the internal units of the model, while M_0 is the total amount of MARCKS in the same units. The axes are logarithmic. The color code represents the number of oscillatory peaks and is therefore a measure for the intensity of the oscillatory effect.

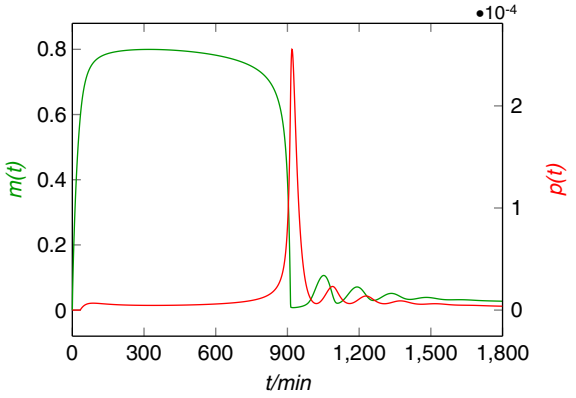

Fig. 7. Simulation of the system directly at the cut off in Fig. 6. The green curve is the amount of membrane bound MARCKS, dependent on time, $m(t)$ and the blue curve is the amount of membrane bound PKC, dependent on time, $p(t)$, which is presented at a different scale.

effect, reducing the periodic time for increasing amounts of MARCKS. The shift to higher periodic times at the lower boundary of the oscillatory area is most likely artificial. It is caused by the increase of the periodic time near the end of an oscillation, when the amplitudes are very low and the system variables change slowly. In Fig. 8b the dependence of the damping constant of the oscillation on the initial conditions is presented. The damping constant increases with an increasing concentration of PKC, which are intuitively clear since more unphosphorylated MARCKS are consumed in the presence of a higher PKC concentration. Further implications of this diagram should be treated with care, as the determination of the damping constant contains some errors, which is hard to avoid since an exact determination of this value needs more parameters than available for the most part of the phase.

4.3. Variation of parameters

Some parameters, used for the model, could not be determined without uncertainties. Therefore, their impact on the oscillatory behavior is studied in more detail (see Fig. 9). Here, all parameters are hold constant at the values given in Table 1, and the parameter of interest is varied around its normal value. The x-axis, which gives the value of the respective parameter, is logarithmically scaled. The examined parameters are the velocity of the reorganization of the membrane k_θ (first line in Fig. 9), the membrane state for which the PKC binding is half of its maximum K_2 (second line), and the amount of membrane bound MARCKS for which the phosphorylation activity of membrane bound PKC is half of its maximum S_0 (third line).

For variation of k_θ, the number of peaks stays constant over an order of magnitude. An increase of k_θ in this range yields a higher frequency and a higher damping coefficient of the oscillation. Thereby, the periodic time is nearly halved, and the damping coefficient increases by a factor of about 0.3 in the range of this parameter variation. Thus, the velocity of the reorganization of the membrane has a direct influence on the oscillatory behavior, but does not significantly alter its occurrence over a broad range.

The parameter K_2 specifies at which the value of the membrane state θ the attachment rate of PKC is half of its maximum. It modulates the amount of PKC required for an oscillatory effect, as less amount of PKC will bind to the membrane for a higher value of K_2. Furthermore, it modulates the alteration rate of the PKC attachment rate with respect to θ. Hence, a change of the parameter K_2 modifies the behavior of the system, even when it is balanced with a change of the total PKC concentration P_0. The intensity of the oscillation is highly dependent on the exact value of K_2. An increase of the parameter K_2 yields to higher periodic times and to lower damping constants. This corresponds to the observations in the phase diagrams that a decrease of PKC concentration yields to higher periodic times and lower damping constants of the oscillation.

For values below $S_0 = 0.01$ the exact value of S_0 is not important, as each graph is nearly constant in this status. This low dependency can be explained by the protein concentration during the oscillation being in a range, in which the enzymatic activity of PKC is saturated. When the value of S_0 exceeds a certain level, it causes the enzymatic activity of PKC to shrink under saturation level near the minima of the oscillation, which negatively affects the intensity of the oscillation. In this region, the periodic time decreases slightly with the increase of S_0, while the damping constant increases significantly. The behavior of these two observables for large values of S_0 should be interpreted carefully, since additional effects gain importance, if only two peaks are analyzed.

4.4. Considering the open system

So far a closed system is considered, where the reactants are exhausted during the regarded process. However, living cells are open systems, in which phosphorylated MARCKS becomes unphosphorylated by phosphatases and is able to rebind at the cell membrane. Thus it is interesting to study the already described MARCKS–PKC-membrane interaction as an open system. As a simplifying approximation, the concentration of the reactants in the subphase can be assumed as constant [2]. This could be called an ideal open system and is an oversimplification of real cellular processes. This approximation neglects the diffusion and is therefore suited to estimate the effects of diffusion on the above treated reaction–diffusion equations.

Since the concentration of the reactants is constant over time, only the interaction between the membrane and the small layer of subphase ($0 \le z \le l$) near the membrane is considered. This sheet has a steady amount of MARCKS and PKC, which corresponds to the total amount of MARCKS M_0 and PKC P_0 in the subphase. Due to the steady supply

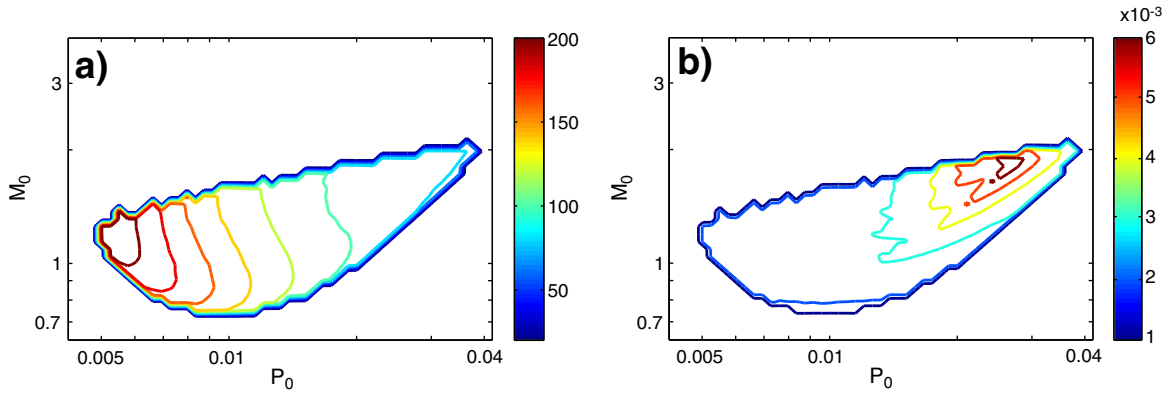

Fig. 8. Periodic time a) and damping constant b) of the oscillation depending on the amount of MARCKS M_0 and PKC P_0. The axes are logarithmic.

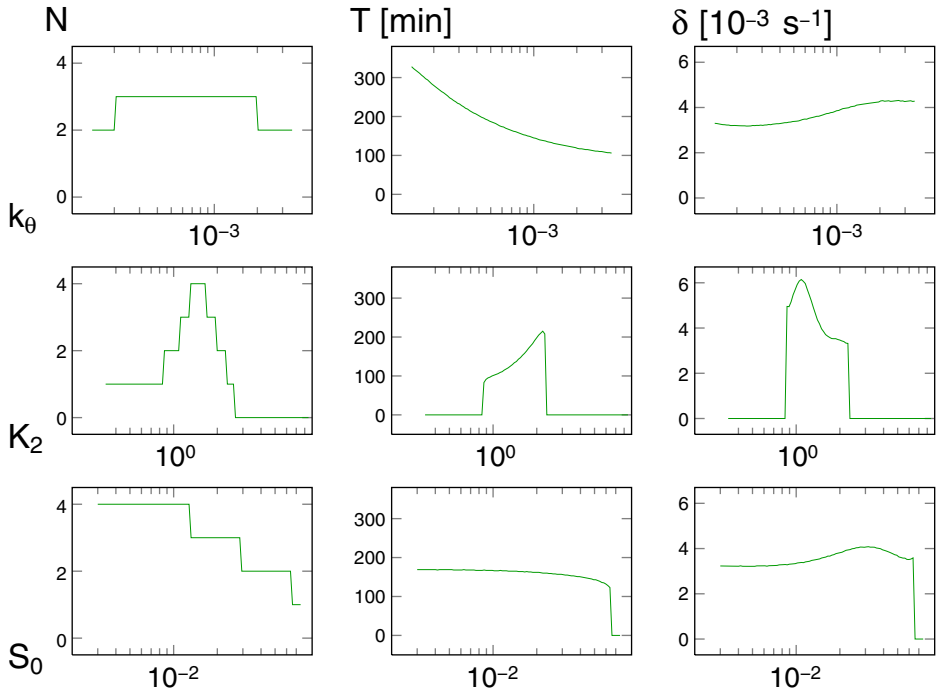

Fig. 9. Change of the oscillation observables by variation of row 1: k_θ, row 2: K_2 and row 3: S_0. The left column illustrates the number of peaks N, the middle column the periodic time T and the right column the damping constant δ, depending on the change of the variables.

of reactants, the MARCKS–PKC-membrane system can perform an undamped oscillation.

Phase diagrams for the open system were generated analogously to the phase diagrams for the closed system. Fig. 10 shows the periodic time depending on the total amount of MARCKS M_0 and PKC P_0 in the subphase. It becomes clear, that oscillations arise only at certain conditions. The behavior of the system outside of the oscillatory domain is, in general, similar to the closed system. It is noticeable that periodic time decreases toward the inside of the oscillatory region. For the closed system, with its damped oscillation, the number of peaks was used as a measure for the intensity of the oscillation. This approach is questionable for the open system, where undamped oscillations are possible. Here, the number of oscillations in a given time is largely dependent on the periodic time.

The damping constant for different total amounts of MARCKS M_0 and PKC P_0 in the subphase is illustrated in Fig. 11. For low amounts of MARCKS the oscillation is damped. As a general trend, it can be seen that lower amounts of MARCKS and higher amounts of PKC enhance the damping. However, there is an area in the phase space, where an increase in the PKC concentration reduces the damping constant. Above a certain level of MARCKS, which is dependent on the amount of PKC, there is no measurable damping constant. The system performs an undamped oscillation in this region. In comparison with the phase diagrams of the closed system, the cut off line is missing in the open system.

4.5. Stability analysis

The first aim of a stability analysis is the identification of critical points (or equilibrium points) in the system. The closed system with MARCKS and PKC (Eq. (1)) has only one true equilibrium point. The membrane state θ is truly larger than zero. Therefore, at an equilibrium

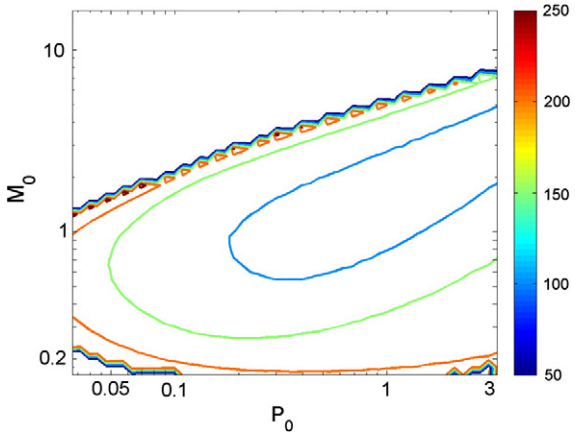

Fig. 10. Phase diagram of the periodic times of the MARCKS–PKC oscillation in an open system. The axes are logarithmic.

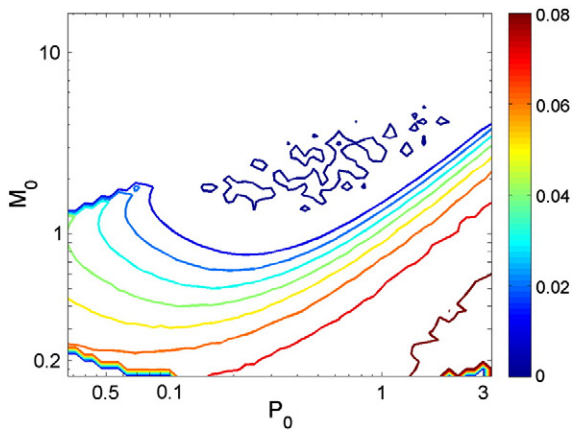

Fig. 11. Damping constant of the MARCKS–PKC oscillation in an open system. The axes are logarithmic.

state, MARCKS and PKC are attached to the membrane. If both types of molecule are attached to the membrane, PKC will phosphorylate MARCKS molecules, producing phosphorylated MARCKS and thereby changing the state of the system. This suppresses any state of a closed system with unphosphorylated MARCKS and PKC for being a critical point. Thus, if PKC is added to a system with MARCKS and membrane containing acidic lipids like PIP_2; only the asymptotic state, in which all MARCKS molecules are phosphorylated, can be an equilibrium point. At this critical point, the phosphorylated MARCKS molecules are equally distributed in the subphase, the PKC molecules in an attachment detachment equilibrium between membrane bound PKC, and equally distributed PKC in the subphase. This state is attractive as the proportion of unphosphorylated MARCKS decreases strictly monotonous over time. Furthermore, the diffusion has the tendency to smooth out inhomogeneities which leads to equally distributed PKC and phosphorylated MARCKS in the subphase. Obviously, the amount of membrane bound PKC $p(t)$ is, without other influences, attracted to a chemical equilibrium of attachment and detachment.

Consequently, the closed system has only one true critical point — the equilibrium state with no unphosphorylated MARCKS left in the system. However, it is noticeable by analyzing the simulations that the system seems to be attracted to a state, where it is constant beside the effects of phosphorylation. In order to analyze this behavior, the open system is studied, because in an open system the supply of unphosphorylated MARCKS allows for other critical points. The evolution of the membrane associated variables for an open system is described by the following equations.

$$\begin{aligned}
\dot{m}(t) &= \theta\ k_m^+ M_0 - k_m^- m(t) - \frac{v_{max} p(t) m(t)^{n_p}}{S_0^{n_p} + m(t)^{n_p}} \\
\dot{p}(t) &= \frac{k_p^+\ \theta^4}{K_2^4 + \theta^4} P_0 - k_p^- p(t) \\
\theta &= (1-m(t))(1-p(t))\theta_{st}(t) \\
\theta_{st}(t) &= k_\theta \left(\sqrt{(A_{dis}(m(t))} - \theta_{st} \right).
\end{aligned} \tag{8}$$

This system was treated for different conditions, on a vertical cut through the phase diagram (see Fig. 11). For $M_0 = 0.5$ and $P_0 = 0.5$, the system has one equilibrium point at the following phase space coordinates:

$$\begin{aligned}
m_c &= 0.024 \\
p_c &= 4.7 * 10^{-5} \\
\theta_c &= 0.13.
\end{aligned} \tag{9}$$

A linear stability analysis yields the highest Lyapunov exponent l_1, which is given below:

$$l_1 = -2.3 * 10^{-4} \tag{10}$$

where the Lyapunov exponent was approximated with an evolution time frame of $\tau = 10^{10}\ s$. The largest Lyapunov exponent is smaller than zero, which states that the critical point is stable under these conditions. Thus, trajectories close to the equilibrium point are attracted to it. This leads to a damping effect in the long term behavior of the system. The damping constant of a normal mode can be calculated with the equation $\kappa_i = -\ln(|\lambda_i|)$ [46] and yields $\kappa_1 = 0.014$. It is considerably smaller than the damping constant in the simulation with $\kappa = 0.027$. This mismatch is mainly caused by influences from the other normal modes, which have a significantly larger damping constant of $\kappa_{2/3} = 0.30$.

For a higher MARCKS concentration of $M_0 = 1.5$ and the same amount of PKC $P_0 = 0.5$, the system has one critical point as well. Its phase space coordinates and the results of the stability analysis are given below, whereby the Lyapunov exponent was again approximated with an evolution time frame of $\tau = 10^{10}\ s$.

$$\begin{aligned}
m_c &= 0.056 \\
p_c &= 1.9 * 10^{-4} \\
\theta_c &= 0.19 \\
l_1 &= 1.3 * 10^{-3}.
\end{aligned} \tag{11}$$

The fact that the largest eigenvalue of the propagator λ_1 is larger than one, and the highest Lyapunov exponent is larger than zero, indicates an instability of the critical point. This means that near the critical point perturbations get amplified in the direction of v_1. In principle, this could lead to chaotic behavior, where the effect of perturbations builds up endlessly. However, the significance of the above statements are restricted to a small range around the equilibrium point within the linear approximation is valid. Outside of the range of validity, the saturation of the membrane limits the build-up of the chaotic behavior. This unstable critical point corresponds to the undamped oscillations in the open system.

For a significant higher amount of MARCKS $M_0 = 5$ and the same amount of PKC $P_0 = 0.5$, the system has three critical points. Their phase space coordinates and their highest Lyapunov exponent, which is estimated with an evolution time frame of $\tau = 10^{10}\ s$, are given below.

$$\begin{array}{lll}
m_{c1} = 0.17 & m_{c2} = 0.60 & m_{c3} = 0.83 \\
p_{c1} = 0.0010 & p_{c2} = 6.7 * 10^{-4} & p_{c3} = 4.4 * 10^{-5} \\
\theta_{c1} = 0.29 & \theta_{c2} = 0.26 & \theta_{c3} = 0.13 \\
l_{c1} = 0.0014 & l_{c2} = 8.3 * 10^{-4} & l_{c3} - 6.2 * 10^{-4}
\end{array} \tag{12}$$

The first two critical points are unstable, while the third point with the highest amount of membrane bound MARCKS is stable. It corresponds to a saturation of the membrane with MARCKS, whereby the low amount of membrane bound PKC slightly modifies the detachment rate of MARCKS. In the simulation, the system reaches the stable third equilibrium point after about 100 min, and stays there without a transient oscillation. The first critical point corresponds to the critical point of the second stability analysis (see Eq. (11) and the following). The second critical point might be corresponding to the intermediate state in the closed system, which is discussed in Section 4.2. However, it is also possible that the intermediate state of the closed system correspond to a stable state in the open system. Thereby the steady consumption of unphosphorylated MARCKS in the closed system would decrease the value of M_0 until the 'critical point' vanishes.

By further increasing the amount of MARCKS in the subphase, a change in the behavior of the stability analysis is noticeable. By a value of $M_0 = 8$, only the stable critical point of the above discussed coordinates is preserved. The critical point and its Lyapunov exponent are given below, whereby an employed time of $\tau = 10^{10}\ s$ was used for the estimation of the Lyapunov exponent.

$$\begin{aligned}
m_c &= 0.90 \\
p_c &= 6.8 * 10^{-6} \\
\theta_c &= 0.083 \\
l_c &= -7.9 * 10^{-4}.
\end{aligned} \tag{13}$$

A simulation of the system with these parameters reaches the stable equilibrium point after about 100 min, and remains constant without a transient oscillation, similar to the case above. By a further increase of the amount of MARCKS, the principle behavior of the system according to the stability analysis does not change. In all the above examples, the amount of PKC in the subphase was constant. It is noticeable that in all these examples a higher amount of PKC on the membrane at a critical point corresponds to a higher Lyapunov exponent and thus a more unstable critical point. In summary, the system is robust toward small variations in the amount of proteins involved; however, extensive changes can alter its behavior.

5. Discussion and relevance to biological systems

In the present work, a model was developed, allowing to determine the experimental conditions, at which the attachment/detachment cycle of MARCKS and PKC on a lipid membrane is detectable in form of an oscillatory behavior of the lateral pressure. This cycle – the ME-switch – is an important part of signal transduction processes. In order to regulate different signal transduction pathways, the ME-switch is responsible for the local availability of PIP_2 [29,5,47]. In this respect, the motivation of our work was to achieve a better understanding of this biological mechanism. The realization of such complex biological processes in vivo is very difficult, thus we have to find simplifications in the experiments as well as in the theoretical modeling. Hereby it is beneficial if mathematical models are based on experimentally well-studied systems. In this way, parameters and rate constants can be taken from experimental results to allow for predictions of the investigated system. An emphasis of this work was to determine the attachment/detachment rates and the phosphorylation of MARCKS by PKC, as well as the parameters of these reactions as realistic as possible. The changing membrane structure and its influence on the attachment rates were considered thoroughly. Furthermore, the long standing assumption that PIP_2 is enriched in the disordered phase of a lipid membrane was verified with fluorescence microscopy. These efforts substantiate the proposed mechanism for the occurring oscillations. Based on the good emulation of the experimental behavior of the system, meaningful predictions were made in the form of phase diagrams. They describe the oscillatory behavior, such as the number of peaks, the periodic time and the damping constant depending on the amounts of MARCKS and PKC. These phase diagrams provide a basis for further investigations of the behavior of the ME-switch. The phase diagrams also revealed a previously unexpected intermediate state, prior to the oscillations.

It is worth mentioning, that the described oscillation can also be observed in an open system that disregards diffusion. This yields the result that the studied oscillation is not caused by the classical formalism of pattern formation of a reaction–diffusion system. It can be understood as a global density oscillation, caused by structural changes of the membrane, depending on the concentration of bound proteins. Furthermore, it is important, that the attachment rates (and/or the detachment rates) of the proteins are dependent on the membrane structure, and that one reactant acts as activator and one as inhibitor. The dependency of the inhibitor on the membrane structure has to be larger than the dependency of the activator. Under these conditions the reactions on the membrane are sufficient for a density oscillation. The diffusion terms in the reaction–diffusion equations act only as modulating terms and are not required for the oscillation. For this reason a new mechanism of temporal pattern formation in biological systems is described. Contrary to a classical reaction–diffusion pattern formation, this mechanism has no inherent length and time scales and produces homogeneous, temporal density oscillations on a membrane, rather than spatial patterns on this membrane.

It is possible that a MARCKS–PKC-membrane system can perform a classical pattern formation, caused by a reaction–diffusion system like proposed by John et al. [26]. For the current model another driving feature emerged, because the main basis for the model was the observation of a variable characterizing the complete membrane.

The simulations of the open system point out, that the existence of the oscillations is not dependent on the system size, as they also occur in systems with no inherent size. This means that the experimental oscillations are in principle applicable on systems with a much smaller size than the experiment, like living cells. One should be cautious about applying these results to biological systems, though. The basic assumption of this model is the existence of different domains of lipids in the membrane, and their dependence on the amount of bound proteins. Furthermore, the active lipid has to be associated with one of these domain types. Finally, a change of the proportion of this 'active domain' by binding of the activator has to have an influence on the activity of the inhibitor. Artificial membranes, such as bilayers and vesicles, can be prepared in a way that these conditions are fulfilled and the current model is applicable. On the other hand, with the concept of 'patchy biological membranes' [16] and lipid rafts in mind it seems possible that these conditions could also be satisfied for certain biological systems.

Even if all of the above requirements are fulfilled, a biological system has significantly different conditions than the experiments, which were modeled in this work. In the experiments, the occurring phenomenons had to be amplified to make them measurable despite the noise. Biological membranes have a PIP_2 concentration of 1–5%, in contrast to the 10% in the experiments [6]. This severely increases the detachment rates. Furthermore, in biological membranes a phase separation between liquid ordered and liquid disordered domains occurs, rather than phase separation between a fluid phase and a crystalline phase. This should increase the velocity of reorganization in the membrane. These variations significantly reduce the periodic time of potential oscillations. The periodic time of possible biological MARCKS–PKC oscillations is in the range of minutes rather than hours. This rough estimate fits well to the measured time frame of the ME-switch by Thelen et al. [44].

Under physiological conditions, other cell components would influence the described density oscillation of MARCKS and PKC at lipid membranes. In this regard calmodulin could play a major role for the treated system. It is classically thought that calcium-activated calmodulin (Ca^{2+}/CaM) translocates MARCKS from the membrane, by binding to its effector domain. This process is mutual exclusive with the phosphorylation of MARCKS by PKC and not directly dependent on the structure of the membrane as Ca^{2+}/CaM does need further activation by lipids to bind to membrane associated MARCKS molecules [3,6]. Thus, the effect of Ca^{2+}/CaM would only enter our model as a variation of the detachment constant of MARCKS. A change in the level of calmodulin or calcium could regulate and vary the described temporal pattern of MARCKS and PKC. It is even conceivable that phenomena like calcium oscillations could induce coupled oscillations. On the other hand, it has been reported that calmodulin colocalizes with MARCKS at the plasma membrane in smooth muscle cells at the (low) calcium resting level [18]. The PKC induced phosphorylation is in this case able to detach MARCKS and calmodulin from the membrane, whereby calmodulin detaches first. This suggests that at a low level of calcium, calmodulin has only a minor effect on the interactions between MARCKS, PKC and the plasma membrane. Therefore it seems likely that calmodulin would hardly influence the here described density oscillations, in a system with a low calcium level.

The present model is not inherently limited to the MARCKS–PKC system. The reported formalism of temporal pattern formation could be an example of a broader class of temporal pattern forming, membrane associated, activator–inhibitor systems. A potential example is gelsolin, which is a regulator of the cortical actin network. Like MARCKS, it binds on PIP_2 and its phosphorylation by PKC (or in this case $PP60^{c-src}$, respectively) is enhanced in the presence of PIP_2 [49,10].

A conformation by further studies that the results of this work are applicable for biological membranes would significantly improve our understanding of the myristoyl-electrostatic switch, associated with a generally improved understanding of signal transduction processes. The ME-switch affects the calcium level of the cell, as well as the amount of available phosphatidylinositol lipids, which both have significant influence on multiple cellular processes. A potential partly dynamic behavior of the ME-switch could alter the view on this process. It could be connected to already observe calcium waves [30] and calcium oscillations [7], which are important in gene expression [13].

Acknowledgements

We would like to thank Marcus Bär and Sergio Alonso for the helpful discussions. This work was funded by the Sächsische Forschergruppe 'From Local Constraints to Macroscopic Transports' (SFG 877).

References

[1] O. Albrecht, H. Gruler, E. Sackmann, Polymorphism of phospholipid monolayers, J. Phys. Fr. 39 (3) (1978) 301–313.
[2] S. Alonso, U. Dietrich, C. Händel, J.A. Käs, M. Bär, Oscillations in the lateral pressure of lipid monolayers induced by nonlinear chemical dynamics of the second messengers MARCKS and protein kinase C, Biophys. J. 100 (2011) 939–947.
[3] A. Arbuzova, J. Wang, D. Murray, J. Jacob, D.S. Cafiso, S. McLaughlin, Kinetics of interaction of the myristoylated alanine-rich c kinase substrate, membranes, and calmodulin, J. Biol. Chem. 272 (1997) 27167–27177.
[4] A. Arbuzova, D. Murray, S. McLaughlin, MARCKS, membranes, and calmodulin: kinetics of their interaction, Biochim. Biophys. Acta 1376 (1998) 369–379.
[5] A. Arbuzova, L. Wang, J. Wang, G. Hangyás-Milháyné, D. Murray, B. Honig, S. McLaughlin, Membrane binding of peptides containing both basic and aromatic residues. experimental studies with peptides corresponding to the scaffolding region of caveolin and the effector region of MARCKS, Biochem. J. 39 (2000) 10330–10339.
[6] A. Arbuzova, A.A.P. Schmitz, G. Vergères, Cross talk unfolded: MARCKS proteins, Biochem. J. 362 (2002) 1–12.
[7] M.J. Berridge, A. Galione, Cytosolic calcium oscillators, FASEB J. 2 (1988) 3074–3082.
[8] A. Blume, A comparative study of the phase transitions of phospholipid bilayers and monolayers, Biochim. Biophys. Acta 557 (1979) 32–44.
[9] E.A. Clark, J.S. Brugge, Integrins and signal transduction pathways: the road taken, Science 2680 (5208) (1995) 233–239.
[10] V. de Corte, J. Gettemans, J. Vandekerckhove, Phosphatidylinositol 4,5-bisphosphate specifically stimulates PP60c-src catalyzed phosphorylation of gelsolin and related actin-binding proteins, FEBS Lett. 401 (1997) 191–196.
[11] U. Dietrich, P. Krüger, T. Gutberlet, J.A. Käs, Interaction of the MARCKS peptide with PIP_2 in phospholipid monolayers, Biochim. Biophys. Acta 1788 (2009) 1474–1481.
[12] U. Dietrich, P. Krueger, J.A. Kaes, Structural investigation on the adsorption of the MARCKS peptide on anionic lipid monolayers — effects beyond electrostatic, Chem. Phys. Lipids 164 (2011) 266–275.
[13] R.E. Dolmetsch, K. Xu, R.S. Lewis, Calciumoscillations increase the efficiency and specificity of gene expression, Nature 392 (1998) 933–936.
[14] D.R. Dries, A.C. Newton, Kinetic analysis of the interaction of the C1 domain of protein kinase C with lipid membranes by stopped-flow spectroscopy, J. Biol. Chem. 283 (2008) 7885–7893.
[15] S.L. Duncan, R.G. Larson, Comparing experimental and simulated pressure–area isotherms for DPPC, Biophys. J. 94 (2008) 2965–2986.
[16] D.M. Engelman, Membranes are more mosaic than fluid, Nature 438 (2005) 578–580.
[17] R. Erban, S.J. Chapman, Reactive boundary conditions for stochastic simulations of reaction–diffusion processes, Phys. Biol. 4 (2007) 16–28.
[18] C. Gallant, J.Y. You, Y. Sasaki, Z. Grabarek, K.G. Morgan, MARCKS is a major PKC-dependent regulator of calmodulin targeting in smooth muscle, J. Cell Sci. 180 (16) (2005) 3595–3605.
[19] A. Gierer, H. Meinhardt, A theory of biological pattern formation, Kybernetik 12 (1972) 30–39.
[20] M. Glaser, S. Wanaski, C.A. Buser, V. Boguslavsky, W. Rashidzada, A. Morris, M. Rebecchi, S.F. Scarlata, L.W. Runnels, G.D. Prestwich, J. Chen, A. Aderem, J. Ahn, S. McLaughlin, Myristoylated alanine-rich C kinase substrate (MARCKS) produces reversible inhibition of phospholipase C by sequestering phosphatidylinositol 4,5-biphosphate in lateral domains, J. Biol. Chem. 271 (42) (1996) 26184–26193.
[21] J.M. Graff, J.I. Gordon, P.J. Blackshear, Myristoylated and nonmyristoylated forms of a protein are phosphorylated by protein kinase C, Science 246 (1989) 503–506.
[22] J.M. Graff, R.R. Rajan, R.R. Randall, A.C. Nairn, P.J. Blackshear, Protein kinase C substrate and inhibitor characteristics of peptides derived from the myristoylated alanine-rich C kinase substrate (MARCKS) protein phosphorylation site domain, J. Biol. Chem. 266 (1991) 14390–14398.
[23] E. Haleva, N. Ben-Tal, H. Diamant, Increased concentration of polyvalent phospholipids in the adsorption domain of a charged protein, Biophys. J. 86 (4) (2004) 2165–2178.
[24] J.H. Hartwig, M. Thelen, A. Rosen, P.A. Janmey, A.C. Nairn, A. Aderem, MARCKS is an actin filament crosslinking protein regulated by protein kinase C and calcium–calmodulin, Nature 356 (1992) 618–622.
[25] L. He, B. Niemeyer, A novel correlation for protein diffusion coefficients based on molecular weight and radius of gyration, Biotechnol. Prog. 19 (2003) 544–548.
[26] K. John, M. Bär, Travelling lipid domains in a dynamic model for protein-induced pattern formation in biomembranes, Phys. Biol. 2 (2005) 123–132.
[27] K.J. Klopfer, T.K. Vanderlick, Isotherms of dipalmitoylphosphatidylcholine (DPPC) monolayers: features revealed and features obscured, J. Colloid Interface Sci. 182 (1996) 220–229.
[28] S. Kondo, T. Miura, Reaction–diffusion model as a framework for understanding biological pattern formation, Science 329 (5999) (2010) 1616–1620.
[29] T. Laux, K. Fukami, M. Thelen, T. Golub, D. Frey, P. Caroni, GAP43, MARCKS, and CAP23 modulate $PI(4,5)P_2$ plasmalemmal rafts, and regulate cell cortex actin dynamics through a common mechanism, J. Cell Biol. 149 (7) (2000) 1455–1471.
[30] J. Lechleiter, S. Girard, E. Peralta, D. Clapham, Spiral calcium wave propagation and annihilation in Xenopus laevis oocytes, Science 252 (1991) 123–126.
[31] M.H. Lee, R.M. Bell, Mechanism of protein kinase C activation by phosphatidylinositol 4,5-bisphosphate, Biochem. J. 30 (1991) 1041–1049.
[32] M.H. Lee, R.M. Bell, Supplementation of the phosphatidyl-L-serine requirement of protein kinase C with nonactivating phospholipids, Biochem. J. 31 (22) (1992) 5176–5182.
[33] I. Levental, P.A. Janmey, A. Cebers, Electrostatic contribution to the surface pressure of charged monolayers containing polyphosphoinositides, Biophys. J. 95 (2008) 1199–1205.
[34] M. Loose, E. Fischer-Friedrich, J. Ries, K. Kruse, P. Schwille, Spatial regulators for bacterial cell division self-organize into surface waves in vitro, Science 320 (2008) 789–792.
[35] H.-H. Lu, Y.-M. Yang, J.-R. Maa, On the induction criterion of the marangoni convection at the gas/liquid interface, Ind. Eng. Chem. Res. 36 (2) (1997) 474–482.
[36] S. McLaughlin, A. Aderem, The myristoyl-electrostatic switch: a modulator of reversible protein-membrane interactions, Trends Biochem. Sci. 20 (1995) 272–276.
[37] S. McLaughlin, J. Wang, A. Gambir, D. Murray, PIP_2 and proteins: interactions, organization, and information flow, Annu. Rev. Biophys. Biomol. Struct. 31 (2002) 151–175.
[38] D. Murray, A. Arbuzova, B. Honig, S. McLaughlin, The role of electrostatic and nonpolar interactions in the association of peripheral proteins with membranes, Curr. Top. Membr. 52 (2002) 277–307.
[39] E.A. Nalefski, A.C. Newton, Membrane binding kinetics of protein kinase C betaII mediated by the C2 domain, Biochem. J. 40 (2001) 13216–13229.
[40] Y. Nishizuka, Protein kinase C and lipid signaling for sustained cellular responses, FASEB J. 9 (7) (1995) 484–496.
[41] S. Ohmori, N. Sakai, Y. Shirai, H. Yamamoto, E. Miyamoto, N. Shimizu, N. Saito, Importance of protein kinase C targeting for the phosphorylation of its substrate, myristoylated alanine-rich C-kinase substrate, J. Biol. Chem. 275 (2000) 26449–26457.
[42] P.H. Richter, M. Eigen, Diffusion controlled reaction rates in spheroidal geometry: application to repressor–operator association and membrane bound enzymes, Biophys. Chem. 2 (1974) 255–263.
[43] S. Soh, M. Byrska, K. Kandere-Grzybowska, B.A. Grzybowski, Reaction–diffusion systems in intracellular molecular transport and control, Angew. Chem. 122 (2010) 4264–4294.
[44] M. Thelen, A. Rosen, A.C. Nairn, A. Aderem, Regulation by phosphorylation of reversible association of a myristoylated protein kinase C substrate with the plasma membrane, Nature 351 (1991) 320–322.
[45] A.M. Turing, The chemical basis of morphogenesis, Philos. Trans. R. Soc. Lond. Ser. B Biol. Sci. 237 (1952) 37–72.
[46] H. von Storch, G. Bürger, R. Schnur, J.S. von Storch, Principal oscillation patterns: a review, J. Clim. 8 (1995) 377–400.
[47] J. Wang, A. Arbuzova, G. Hangás-Milháyné, S. McLaughlin, The effector domain of myristoylated alanine-rich C kinase substrate binds strongly to phosphatidylinositol 4,5-biphosphate, J. Biol. Chem. 276 (2001) 5012–5019.
[48] J. Wang, A. Gambhir, G. Hangyás-Mihályné, D. Murray, U. Golebiewska, S. McLaughlin, Lateral sequestration of phosphatidylinositol 4,5-biphosphate by the basic effector domain of myristoylated alanine-rich C kinase substrate is due to nonspecific electrostatic interactions, J. Biol. Chem. 277 (2002) 34401–34412.
[49] F.X. Yu, H.Q. Sun, P.A. Janmey, H.L. Yin, Identification of a polyphosphoinositide-binding sequence in an actin monomer-binding domain of gelsolin, J. Biol. Chem. 267 (1992) 14616–14621.